Astron. Astrophys. 322, 291–295 (1997)

ASTRONOMY
AND
ASTROPHYSICS

Mode switching of the water maser in OH 39.7+1.5

D. Engels[1], **A. Winnberg**[2], **C.M. Walmsley**[3], **and J. Brand**[4]

[1] Hamburger Sternwarte, Gojenbergsweg 112, D-21029 Hamburg, Germany
[2] Onsala Space Observatory, S-43992 Onsala, Sweden
[3] I. Physikalisches Institut, Universität zu Köln, Zülpicherstr. 77, D-50937 Köln, Germany
[4] Istituto di Radioastronomia, C.N.R., Via Gobetti 101, I-40129 Bologna, Italy

Received 16 October 1996 / Accepted 22 November 1996

Abstract. Monitoring of the H_2O maser in OH 39.7+1.5 as well as spatial interferometry show clear evidence that the maser switches occasionally its beaming direction between radial and tangential paths in step with the stellar pulsation cycle. Outside the minimum, several radially beamed maser features are present, which are absent ($\leq$ 20 mJy) during the minimum. Competition between gain paths causes tangentially beamed maser emission only to occur, when the temperature in the maser shell is too low to excite radially beamed masers.

The radius of the H_2O maser shell extends between 6 10^{14} cm (40 AU) and at least 3 10^{15} cm (200 AU), with the inner radius probably set by quenching of the maser due to high gas density close to the star. Within the H_2O maser shell, the circumstellar outflow accelerates from v$\approx$9 km s^{-1} up to the terminal expansion velocity of $\approx$18 km s^{-1}. The expansion velocity of the circumstellar shell is constant between the outer radius of the water maser shell and the location of the 1612 MHz OH maser shell at 3 10^{16} cm, showing the absence of strong velocity gradients at large radial distances.

Key words: stars: AGB and post-AGB – masers – stars: individual: OH 39.7+1.5 – radio lines: stars

1. Introduction

OH 39.7+1.5 (AFGL 2290) is an OH/IR star discovered as a bright infrared source by the AFGL-Infrared-Sky-Survey, and subsequently detected as a strong 1612 MHz OH maser by Allen et al. (1977). The star is a long-period variable with a period P = 1430 $\pm$ 24 days at a distance of 0.98 $\pm$ 0.35 kpc (Van Langevelde et al. 1990), and has a stellar radial velocity inferred from the OH maser spectrum of 20 km s^{-1} (Slootmaker et al. 1985).

The water maser in OH 39.7+1.5 was discovered by Marques Dos Santos et al. (1979) and later remeasured by Nyman et al. (1986) and Engels et al. (1986). The latter found that the water maser profile varied in a unique manner, exhibiting a double-peaked profile similar to the 1612 MHz OH maser profiles during the bright phase of the star and a single line close to the stellar radial velocity while the star was dim. Lewis & Engels (1991) suggested that competitive gain between maser gain paths explains this behaviour. Consequently, OH 39.7+1.5 was considered as an important source for a new monitoring campaign, which we started in 1990 to study the H_2O maser variability in various types of stars (Engels et al. 1993). Fortunately, the maser spectrum showed the same kind of change again, enabling a closer study of this phenomenon with the aid of interferometric maps.

Send offprint requests to: D. Engels (dengels@hs.uni-hamburg.de)

2. Observations

Single dish observations of the H_2O maser line at 22 GHz have been made since 1990 with the Effelsberg 100m and Medicina 32m telescopes at typical intervals of a few months. For details on the observational set-ups, we refer to Engels & Lewis (1996), Comoretto et al. (1990), and Brand et al. (1994). The spectra of OH 39.7+1.5 cover more than a full cycle including the minima in 1991 May and 1995 April, and the maximum in 1993 April. A log of the observations is given in Table 1.

Interferometric maps were made with the Very Large Array (VLA)[1] in its A-configuration on four occasions in 1990 February and June, 1991 August (close to minimum), and 1992 December. All 27 antennas were used yielding an angular resolution of 0.″08 at 22 GHz. We chose a receiver bandwidth of 3.125 MHz to obtain a total velocity range of 42 km s^{-1} and the bandwidth was split into 64 channels, yielding a velocity resolution of 1.32 km s^{-1} after on-line Hanning smoothing. Data from right and left circular polarization mode were averaged. Typical integration times were 30 min. on source and 12 min. on the phase calibrator 1923+210 with a sampling time of 30 sec. Flux calibration was obtained relative to 3C286, and 3C84 was used to calibrate the bandpass.

[1] The VLA is part of National Radio Astronomy Observatory, which is operated by Associated Universities Inc., under cooperative agreement with the National Science Foundation of the USA.

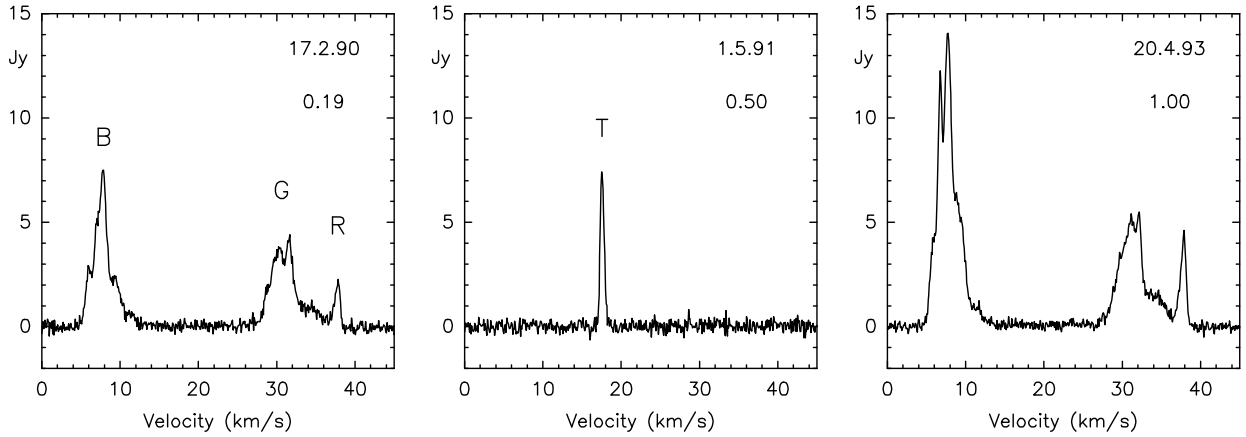

Fig. 1. Representative H_2O maser spectra of OH 39.7+1.5 at three phases (indicated below the date) of its light curve. The major maser features discussed in the text are labeled with capital letters. At phases 0.19 and 1.0, the shape of the profile is of the type we describe as "radial" whereas at phase 0.5, the profile is consistent with tangential amplification.

The data were reduced within AIPS using the spectral line data analysis routines. To improve the sensitivity as well as the dynamic range, self-calibration was applied. In 1991 August the 17.5 km s^{-1} line was used as phase reference and for the other epochs the most blueshifted maser component at 7.5 km s^{-1} was taken. The final sensitivity reached on line-free channels was 13-23 mJy (rms) depending on weather conditions and integration time.

3. Results

3.1. Single-dish observations

Between 1990 and 1995 we obtained 33 single-dish spectra, from which we display three in Fig. 1 to show the general appearance of the maser during this time. During the bright phase of the pulsation cycle the maser consists of three features, one blue- (labeled B in Fig. 1) and the other two redshifted (labeled G(reen) and R(ed)) with respect to the stellar velocity (20 km s^{-1}), each feature being made up of several individual maser lines. The overall shape of the profile is similar to the double-peaked OH profile, and is therefore reminiscent of radially beamed masers in a spherically symmetric expanding circumstellar shell. In the following we refer to these maser features as radial masers. Close to minimum these masers are extinguished, and from the upper limits ($\approx$ 60 mJy (3σ)) of the VLA observation of August 1991 we can infer that the flux densities vary at least a factor 100-1000 during the pulsation cycle.

The spectra during the bright phases in 1990 and 1993 are strikingly similar. Not only did the three maser features reappear in 1993 with a similar shape but also the individual lines contributing to each feature are present in both epochs. The blueshifted feature B, for example, is a blend of 5 individual maser lines, which have within the measuring errors ($\approx$ 0.3 km s^{-1}) the same velocities in 1990 and 1993. This indicates that the radial masers reappeared at exactly the same velocities,

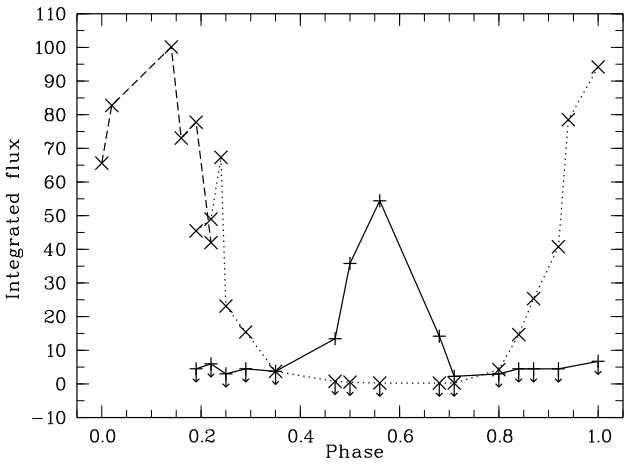

Fig. 2. Integrated fluxes (in 10^{-22} Watt m^{-2}) of the blue (B) feature (x) and of the tangential maser line (+) as function of the phase of the stellar pulsation cycle. For clarity the integrated blue flux is divided by 3. Solid and dotted lines connect data obtained between the maxima in 1990 and 1993, while the dashed line belongs to the following cycle until 1994 March.

after being absent when the star was dim. The velocity range over which H_2O maser emission appears is 5–38 km s^{-1}, almost the same range as displayed by the OH maser (2–38 km s^{-1}; Slootmaker et al. 1985), showing that the most redshifted parts of the H_2O maser have the same outflow velocity as the OH maser shell.

During the weak phase in 1991, when the double-peaked maser had disappeared (at phase $\Phi \sim 0.4$) a new maser line at 17.5 km s^{-1} appeared, reached its maximum at $\Phi \sim 0.6$ and disappeared at $\Phi \leq 0.8$, when the radial masers showed up again. No similar line was observed during the following weak phase in 1995. The new maser is blueshifted by 2.5 km s^{-1} with respect to the stellar velocity and is either a tangentially beamed maser or originates very close to the star, where the

Table 1. Observations at the Effelsberg, Medicina, and VLA radiotelescopes. JD +2440000 is the Julian Date.

Obs. Date	JD	Phase	Tel.	S_I(B)	S_I(T)
		Φ		[10^{-22} W m^{-2}]	
17.02.90	7940	0.19	E	136.5	<4.5
26.02.90	7949	0.20	VLA	–	–
31.03.90	7982	0.22	E	147.0	<6.0
25.04.90	8007	0.24	M	201.9	–
12.05.90	8024	0.25	E	69.3	<3.0
03.06.90	8046	0.27	VLA	–	–
11.07.90	8084	0.29	E	46.2	<4.5
19.10.90	8184	0.35	E	11.1	<3.7
26.10.90	8191	0.36	M	–	–
18.01.91	8275	0.42	M	–	–
30.03.91	8346	0.47	E	<3.0	13.4
30.04.91	8377	0.50	M	–	–
01.05.91	8378	0.50	E	<2.5	35.8
03.08.91	8472	0.56	E	<2.5	54.4
24.08.91	8493	0.58	VLA	–	–
17.01.92	8639	0.68	M	–	–
18.01.92	8640	0.68	E	<2.5	14.2
29.02.92	8682	0.71	E	<2.5	2.5
19.04.92	8732	0.74	M	–	–
05.07.92	8809	0.80	E	12.6	<3.0
01.09.92	8867	0.84	E	44.1	<4.5
15.10.92	8911	0.87	M	75.9	<4.5
22.12.92	8979	0.92	E	122.4	<4.5
28.12.92	8985	0.92	VLA	–	–
27.01.93	9015	0.94	M	235.5	–
20.04.93	9098	1.00	E	282.6	<6.7
21.04.93	9099	0.00	M	196.8	–
13.05.93	9121	0.02	M	248.4	–
02.11.93	9294	0.14	M	300.3	–
30.11.93	9322	0.16	M	219.3	–
17.01.94	9370	0.19	M	233.4	–
08.03.94	9420	0.22	E	126.0	–
16.04.94	9459	0.25	M	66.3	–
28.10.94	9654	0.39	M	7.5	–
18.01.95	9736	0.45	M	–	–
09.03.95	9786	0.48	E	<2.5	<2.5
04.06.95	9873	0.54	E	<2.5	<2.5

outflow velocity is still small. We believe the first one of these possibilities to be true (see below) and refer to this component in the future as "tangential". Apparently we observed a switch from radial to tangential beaming of the maser, correlated with the variability of the star. In Table 1 we list the integrated fluxes of the blueshifted feature (B) and the tangential line (T) for spectra with sufficient S/N, and their temporal variations are shown in Fig. 2. The striking anticorrelation between the radial and the tangential lines strongly suggests that the two beaming directions are mutually exclusive. None of the spectra, taken close to the phases in which the transition must have taken place ($\Phi = 0.35, 0.71,$ and 0.8), showed both lines simultaneously.

3.2. Interferometric observations

Visual inspection of the channel maps showed immediately that we were able to resolve some of the maser features spatially. In particular, feature G (cf. Figs. 1 and 3) is clearly separated into two maser groups with a separation of $\sim 0\farcs1$. At 1 kpc this corresponds to a distance of 1.5 10^{15} cm (100 AU), giving a lower limit for the outer diameter of the H_2O maser shell.

The number of unambiguously identified maser spots in the channel maps is $\approx$15 per epoch and their location is shown in Fig. 3. There is a striking similarity between the maps of the three epochs when radial masers were present. Comparison of individual channel maps between the three epochs show that the radial maser lines came from the same positions in 1990 and 1992. Thus, the maser lines reappear at the same velocity and position after being extinguished close to the minimum of the pulsation cycle. We have to conclude that the velocity structure within the H_2O maser zone giving rise to the radial masers is not altered significantly during one pulsation cycle of the star ($\sim$ 4 years) and that the maser lines reappear as soon as the conditions to pump the maser are restored. This finding is not surprising, because during one period a mass element is able to move only $\approx$2 10^{14} cm outwards, which is small compared to the size of the shell.

The maps of the double-peaked masers are made up, first of all, of maser lines belonging to the blueshifted and the most redshifted feature (labeled B and R in Fig. 1), which are spaced close together and are encircled in Fig. 3. Secondly, there are the maser lines belonging to the G-feature and finally several weak masers located in velocity close to the inner wings of the two maser complexes B and G. The most blue- and redshifted maser lines agree in position on the sky to better than 15 mas, which is strong evidence for radial beaming in an isotropically expanding circumstellar shell. Both maser components define therefore uniquely the line of sight to the star. Averaging over three epochs we find the position of the star to be $\alpha = 18^h\,56^m\,3\fs888\pm0\fs001$, $\delta = 6^\circ\,38'\,49\farcs89\pm0\farcs03$ (1950) coincident within errors with the position obtained from interferometric observations of the OH maser (Bowers et al. 1981). This position is chosen as origin of the maps shown in Fig. 3.

The VLA observation in August 1991 ($\Phi \sim 0.5$) showed maser emission only from the 17.5 km s^{-1} line. Its position is $0\farcs2$ (or 3 10^{15} cm) away from the star, a surprisingly large value compared to the positional spread of the other maser spots. Unfortunately there is no maser spot in this epoch in common with the others, inhibiting a direct alignment of the maps. We cannot exclude the possibility that the large deviation was caused by phase instabilities during the 1991 August observation, although we consider this to be unlikely given the close coincidence ($<$ 20 mas) of the maps for the other three observing periods. The 17.5 km s^{-1} line is therefore clearly off the line of sight to the star and hence we conclude that the beam direction is almost tangential. Because of the relatively large distance from the star, one might question the association of the 17.5 km s^{-1} line with OH 39.7+1.5. However, the striking anti-correlation in variability with the radial masers (Fig. 2) and the observation

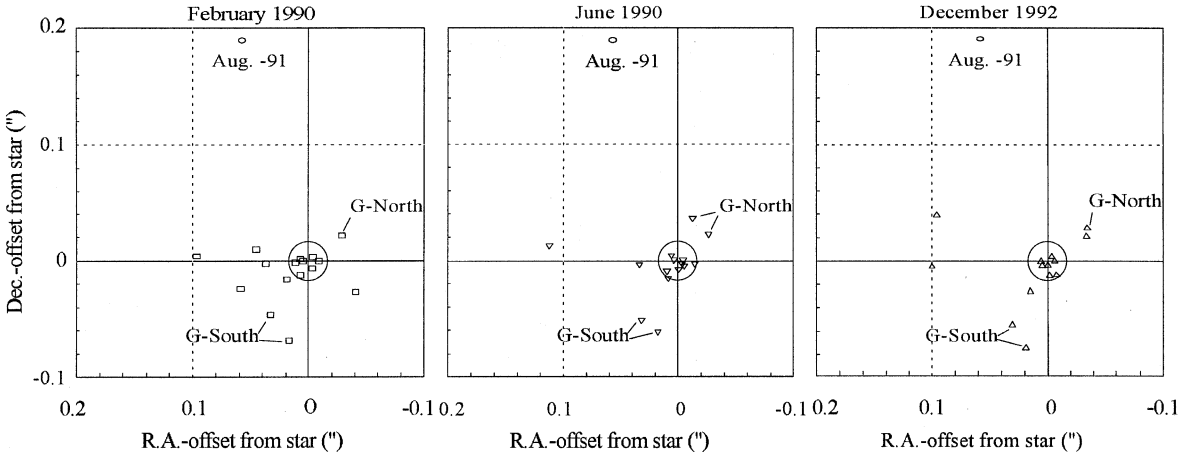

Fig. 3. Location of the maser components identified in the VLA interferometric maps. The position of the tangential maser observed in August 1991 is shown on all of the three maps. Maser components belonging to the features B and R (cf. Fig. 1) are located inside the circle at the origin of the map. Feature G consists of two components, each composed of at least two maser lines.

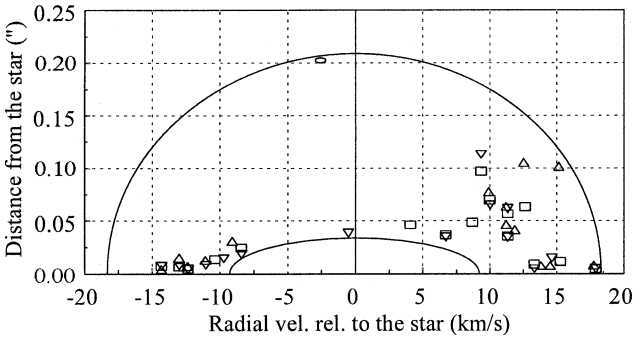

Fig. 4. Radial velocities of H_2O maser components relative to the stellar radial velocity of 20 km s^{-1} plotted against distance of the components from the adopted position of the star. Coding of the maser components denote the different observing epochs: 1990 February (□), 1990 June (▽), 1991 August (o), and 1992 December (△).

of a similar "tangential" maser line (then at 20.6 km s^{-1}) during an earlier pulsation cycle (Engels et al. 1986) prove that the association is real.

Fig. 4 shows a plot of relative velocity against projected radial distance from the star for all maser spots identified in the four epochs. For a thin shell with constant expansion velocity all maser spots are expected to fall close to the locus of a single ellipse. This is not evident here, instead a geometrically thick shell with inner and outer radius of 0.6 and 3 10^{15} cm and inner and outer expansion velocity of 9-10 and 17-18 km s^{-1} is displayed. The existence of an inner radius is probably due to high gas density close to the star, leading to quenching of the maser emission (Cooke & Elitzur 1985) in the inner part of the circumstellar shell. The outer radius, which is set by the largest separation measured for a radial maser and by the location of the tangential maser line, implies an H_2O maser shell size (diameter) of $\geq$400 AU.

The water maser shell for OH 39.7+1.5 lies mostly in the outer part of the acceleration zone of the circumstellar shell, where the velocity gradient is sufficiently small that maser excitation along radial paths occur. As noted in Sect. 3.1 and as is evident from Fig. 4, only the most redshifted H_2O maser velocities reach the terminal expansion velocity given by the OH maser. The B-feature is closely aligned with the R-feature, but has a smaller outflow velocity, implying a position closer to the star. The outer radius, as suggested by Fig. 4, may then give only a lower limit for the maximum size of the water maser shell, because the maser spots determining the outer ellipse in Fig. 4 do not necessarily move with the terminal expansion velocity.

4. Discussion

Previous interferometric measurements of sizes of H_2O maser regions have been restricted to semiregular (SR-), Mira variables and M-Supergiants. OH 39.7+1.5 is the first OH/IR star for which such a measurement has been carried out. Based on the velocities displayed in single-dish spectra, Engels et al. (1986) predicted OH/IR stars to have intermediate sizes between those of the blue AGB variables and those of M-Supergiants. Indeed the outer shell radius of OH 39.7+1.5 of 3 10^{15} cm (200 AU) is about ten times greater than the typical radii of SR- or Mira variables with mass loss rates $\leq 10^{-6}$ $M_\odot$/yr (Bowers & Johnston 1994), and somewhat smaller than in M-Supergiants (Johnston et al. 1985, Bowers et al. 1993, Yates & Cohen 1994). Therefore, in general, the sizes of the H_2O masing region increase with mass loss rate, expansion velocity and probably luminosity of the star.

The most redshifted H_2O maser velocities coincide with the reddest OH maser velocities implying that the final expansion velocity is already reached within the H_2O maser shell. Between the outer radius and the OH maser shell at 3 10^{16} cm (Van Langenvelde et al. 1990) little, if any acceleration of the outflowing gas occurs. Assuming a stellar radius of 2 10^{14} cm and adopting

$3\,10^{15}$ cm as the outer H_2O maser shell radius, the acceleration of the outflow is finished within 15 R_*, followed by a constant expansion over at least 150 R_*. The confinement of the acceleration to the inner part of the shell seems to be a general characteristic of OH/IR stars, given the close coincidence of H_2O and OH maser velocity ranges for many of them (Engels et al. 1986; Engels & Lewis 1996). OH/IR stars show no evidence for large velocity gradients at large radial distances, like the one claimed to be present in the M-Supergiant VX Sgr (Chapman & Cohen 1986). The radial velocity curve is therefore in accordance with the usual theory of radiation pressure on dust, where constant dust opacity beyond the grain condensation radius is assumed (Goldreich & Scoville 1976).

The anticorrelation in the detectability of radial and tangential water masers from OH 39.7+1.5 and their variations is unique, although we have searched for other examples. It was not a singular event for OH 39.7+1.5 however, as a similar line was observed in the past. Apparently, the tangential masers are less stable than the radial ones. While the latter reappear again at the same velocity and position, the former do not. From four periods now covered by observations, tangential lines appeared only during the first (1984) and the third (1991) period, and not during the minima in 1987 (Engels & Lewis 1996) and 1995. Thus observable tangential emission occurs only occasionally.

It is often thought that radial and tangential maser lines are located in different parts of the shell. As small velocity gradients along radial paths are achieved only far away from the star, radial masers are expected to reside in the outer parts of the shell, while the tangential masers are expected preferentially in zones of high velocity gradients close to the star (Chapman & Cohen 1985). However, in the present case masing in the inner acceleration zone is quenched and the spatial position of the tangential line is incompatible with a position in this zone.

It is therefore more plausible to assume that tangential and radial masers come from about the same volume of gas, with tangential emission only possible, as long as radial maser emission is inhibited. During the bright phase of the star, the temperature in the maser shell suffices to collisionally excite the maser throughout the shell and excitation along radial paths will be preferred, because the velocity gradient is smallest in this direction. Pump events will be fully used up by the radial masers, inhibiting maser emission in other directions. When the stellar brightness decreases, the shell temperature decreases and falls eventually below a threshold, beyond which inversion of the maser levels cannot be maintained. The location of this threshold moves radially inward with decreasing shell temperature, shortening the radial maser paths until their lengths become comparable to those possible in other directions. The critical gain length might be estimated from the position and the width of the line profile (0.7 km s^{-1}) of the tangential maser. At a distance of D = $3\,10^{15}$ cm in a constant radially symmetric outflow with v_e = 17 km s^{-1}, velocity coherence $\Delta v \leq 0.7$ km s^{-1} is achieved along a tangential line of sight over a length of D $\Delta v/v_e \approx 10^{14}$ cm. Thus, as soon as the radial gain length approaches this size, the longest gain paths may occur in other directions than the radial one. As even modest asymmetry of the maser zone will produce substantial anisotropy in the outgoing radiation (Alcock & Ross 1985), a switch in beaming direction is possible. The tangential gain length increases until the stellar minimum is reached and decreases afterwards. The temperature variation should have reached a minimum by then, because otherwise the new beaming direction will be extinguished shortly afterwards as well.

Thus considerable fine tuning between the mass loss rate, expansion velocity and luminosity amplitude seems to be required, to make the switch of beaming directions observable. A favourable combination of these parameters may only occur during a short phase of the development of a circumstellar shell, which would explain, why the observation of mode switching is thus far peculiar to OH 39.7+1.5.

Acknowledgements. We like to thank for the support at the VLA, especially E. Brinks, B. Clark, P. and R. Perley, and M. Rupen. We thank Murray Lewis, the referee, for numerous discussions and many suggestions, which helped to improve the paper. The Max-Planck-Institut für Radioastronomie supported this work by ample allocation of observing time and computing facilities. DE was supported by the DFG through travel grants Re 353/25 and En 176/2 and AW acknowledges support by the Swedish Natural Science Research Council. This research made use of the SIMBAD database, operated by CDS in Strasbourg.

References

Alcock C., Ross R.R., 1985, ApJ 290, 433
Allen D.A., Hyland A.R., Longmore A.J., et al., 1977, ApJ 217, 109
Bowers P.F., Johnston K.J., Spencer J.H., 1981, Nat 291, 382
Bowers P.F., Claussen M.J., Johnston K.J., 1993, AJ 105, 284
Bowers P.F., Johnston K.J., 1994, ApJS 92, 189
Brand J., Cesaroni R., Caselli P., et al., 1994, A&AS 103, 541
Chapman J.M., Cohen R.J., 1985, MNRAS 212, 375
Chapman J.M., Cohen R.J., 1986, MNRAS 220, 513
Comoretto G., Palagi F., Cesaroni R., et al., 1990, A&AS 84, 179
Cooke B., Elitzur M., 1985, ApJ 295, 175
Engels D., Schmid-Burgk J., Walmsley C.M., 1986, A&A 167, 129
Engels D., Winnberg A., Brand J., Walmsley C.M., 1993, in: Clegg A., Nedoluha G. (eds.), Astrophysical Masers, Springer, Berlin Heidelberg, p. 403
Engels D., Lewis B.M., 1996, A&AS 116, 117
Goldreich P., Scoville N., 1976, ApJ 205, 144
Johnston K.J., Spencer J.H., Bowers P.F., 1985, ApJ 290, 660
Lewis B.M., Engels D., 1991, MNRAS 251, 391
Marques Dos Santos P., Lépine J.R.D., Gomez Balboa A.M., 1979, AJ 84, 787
Nyman L-Å., Johansson L.E.B., Booth R.S., 1986, A&A 160, 352
Slootmaker A., Herman J., Habing H.J., 1985, A&AS 59, 465
van Langevelde H.J., van der Heiden R., van Schooneveld C., 1990, A&A 239, 193
Yates J., Cohen R.J., 1994, MNRAS 270, 958

This article was processed by the author using Springer-Verlag LaTeX A&A style file *L-AA* version 3.